ARTICLE NO. 80-4111

Stresses in Double-Lap Joints Bonded with a Viscoelastic Adhesive: Part II. Parametric Study and Joint Design

Joyanto K. Sen*
Hindustan Aeronautics Ltd., Bangalore, India
and
Robert M. Jones†
Southern Methodist University, Dallas, Tex.

A parametric study of the behavior of double-lap joints, bonded with a viscoelastic adhesive, is presented in this paper. The study is based on Schapery's Direct Method of viscoelastic stress analysis in the SAAS III finite element program as described in Part I of this paper. In this study, the relative importance of the various material and geometric parameters is quantitatively determined in order to design an efficient joint. The most important parameter is the ratio of the adherend modulus to the equivalent property of the viscoelastic adhesive. The stresses are highest when this ratio is one and decrease as this ratio increases. The next most important parameter is the thickness of the adhesive. With decreasing adhesive thickness, the stress distribution along the length of overlap is increasingly uniform and the gradient of the stress distribution through the adhesive thickness also decreases. The length of overlap influences only the location of the maximum shear stress, whereas a change in the relative thicknesses of the adherends has a minimum influence on the magnitudes of the stresses. The results are all presented in nondimensionalized units so that the criteria for an efficient joint are clearly delineated.

Introduction

THE double-lap joint bonded with a viscoelastic adhesive, as shown in Fig. 1, is analyzed to determine the quantitative influences of the various material and geometric parameters in order to design an efficient joint. The computational tool for the theoretical analysis is the SAAS III finite element program[1] wherein the viscoelastic behavior of the adhesive is incorporated by use of Schapery's Direct Method of transform inversion.[2]

This parametric study is made following good agreement with experimental results of the theoretical results calculated using this finite element model.[3] The adhesive is characterized as linearly viscoelastic and as photoviscoelastically simple, i.e., the principal axes of stress and strain are coincident.[4] Full details of the experimental and theoretical procedures together with the results are presented by Sen.[5]

The influences of the parameters are studied by varying one parameter at a time from a reference joint. The reference joint is the same as joint 1 of Part I of this study,[3] and its parameters are given in Table 1.

The stress distributions presented in this study are nondimensionalized with respect to the applied stress or the nominal shear stress. The axial normal stress σ_y and the tear (normal) stress σ_x are nondimensionalized with respect to the applied stress σ_a. The shear stress τ_{xy} is nondimensionalized with respect to the nominal shear stress:

$$\tau_{\text{nom}} = \sigma_a t_C / c$$

where the notation is given in Fig. 1.

The failure of a double-lap joint, bonded with a viscoelastic adhesive and subjected to a constant load, can occur in any one of four modes in its three elements: 1) shear failure in the adhesive, 2) tear failure where the adhesive is separated from the adjoining adherend, 3) tension failure in the center adherend at $y=\eta/2+c$, and 4) tension failure in the outer adherend at $y=0$. The shear and tear failures in the adhesive can be caused by high stresses or by high creep strain if the load is applied for a very long time. The failure caused by high creep strain will not originate at the interface but very near it. The interface strain is governed by the constant strain in the elastic adherend. A short distance from the interface, a redistribution of the adhesive stresses occurs in order to reflect the constraint on the strain imposed by the adherend. The thickness of the boundary layer of redistributed stresses is less than 4% of the adhesive thickness. The maximum adhesive stresses and strains therefore do not occur at the interface but at a short distance from it.

In an adhesive-bonded joint, the desired mechanism for transfer of the applied load is shear. The ideal joint will be one in which the shear stresses along the interfaces are uniform and there are no tear stresses. In actual joints, tear stresses exist. Thus, the distributions of the shear and tear stresses are nonuniform with high stresses just inside one end,

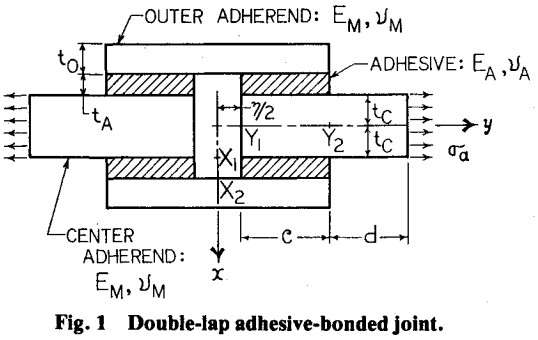

Fig. 1 Double-lap adhesive-bonded joint.

Received May 15, 1979; revision received Feb. 1, 1980.

Index categories: Structural Statics; Materials, Properties of; and Structural Design.

*Assistant Chief Design Engineer, Helicopter Design Bureau.
†Professor of Solid Mechanics. Associate Fellow AIAA.

Table 1 Parameters of the reference joint[a]

Parameter	Magnitude
Adherend modulus, MPa (psi)	68,966 (1×10^7)
Adherend Poisson's ratio	0.33
Overlap length c, mm (in.)	51.05 (2.01)
Overhang length d, mm (in.)	127 (5.00)
Adhesive thickness t_A, mm (in.)	6.81 (0.268)
Center adherend thickness $2t_C$, mm (in.)	25.4 (1.00)
Outer adherend thickness t_O, mm (in.)	6.35 (0.25)
Spacing between center adherends η, mm (in.)	1.52 (0.06)
Model width, mm (in.)	6.35 (0.25)
Applied stress σ_a, MPa (psi)	1.1 (160)

[a]The notation is shown in Fig. 1.

the leading end, of the adherend-adhesive interface. The location of the leading end depends on the joint geometry. If the load path is drawn from the adherend to the adhesive, the leading end of the interface is where the adherend first touches the adhesive. For the two adherends, the adhesive has two leading ends located diagonally across the adhesive thickness. For the outer adherend, the leading end is at $y=\eta/2$, or at $(y-\eta/2)/c=0$. For the center adherend, the leading end is at $y=\eta/2+c$, or at $(y-\eta/2)/c=1$. The other end of the interface, which is not the leading end, is referred to as the trailing end.

The ranges of the parameters which are studied and their respective influences on the stress distributions in the adhesive and adherends are given in the next section. These influences are then discussed in the context of designing an ideal joint. A nondimensionalized joint parameter, the overlap ratio, is suggested for evaluating the merits of various joint design. In addition, the probable failure modes for particular stress distributions are identified.

Numerical Results

The joint is doubly symmetric about the x and y axes, so only one-quarter of the joint is analyzed. The relevant planes along which the stress distributions are presented are shown in Fig. 1. The adhesive interface with the center adherend is at $x=X_1$ and that with the outer adherend is at $x=X_2$. The adhesive free edge at $y=\eta/2$ is identified as $y=Y_1$ and that at $y=\eta/2+c$ is identified as $y=Y_2$.

The influences of the parameters are shown as variations of the stress concentration factors (scf) with the variations of the parameters. The stress distributions in certain cases have been presented as typical examples. The stress distributions satisfy the free boundary conditions of zero stress wherever necessary even though this condition is not shown in the figures. Thus, the shear stress τ_{xy} in the adhesive must be zero at $y=Y_1$ and $y=Y_2$, and the axial normal stress σ_y must be zero at $y=Y_1$ for the center adherend and at $y=Y_2$ for the outer adherend. The finite element analysis does not result in precisely zero magnitudes of the stresses in the elements adjacent to the free boundaries but does result in very small magnitudes of the stresses. The highest magnitude of σ_y at a free boundary element is 2.5% of the applied stress σ_a. The highest magnitude of τ_{xy} at a free boundary element is 5% of the nominal shear stress. These stress distributions when extrapolated across one-half the width of the element to the free boundary will result in nearly zero magnitudes of the stresses. The ranges of the parameters and their respective influences are discussed in what follows.

Parameters

The parameters which influence stress distributions and, hence, the failure mode, in double-lap joints are the mechanical properties of the materials and the geometry of the joint. The mechanical properties are the moduli and the Poisson's ratios. The geometric parameters are the thicknesses of the adherends and the adhesive as well as the lengths of the overlap and the overhang.

The influence of Poisson's ratio on the stress distribution has not been studied because only large changes in Poisson's ratio affect the distributions and magnitudes of the stresses. The range of variation of Poisson's ratio for common adhesive systems is very limited (for most elastic adherend materials ν is around 0.3); thus, only the influence of the material modulus is assessed in this analysis. The adhesive Poisson's ratio is constant at 0.48[3,4] and that of the adherend is 0.33. In this analysis, the same adhesive[3,4] is used in all configurations of the joint studied. The adherend elastic modulus E_M is varied but a constant "representative" adhesive "modulus" E_A is used in comparisons of the influence of the moduli on the stress distributions in the joint. The "modulus" E_A is defined as the magnitude of the relaxation modulus $E_r(t)$ at 10.8 h after loading. In the relaxation modulus - time distribution curve, E_A is on the "viscoelastic" portion of the curve just before the "rubbery" state.[5] The magnitude of E_A is 345 MPa (50,000 psi). The magnitude of E_M is varied such that the range of $E_M/E_A=1,2,4,10,20,200$.

The geometric parameters, Fig. 1, are varied to include those magnitudes of the parameters which greatly influence the distributions and magnitudes of the stresses. All but one of the geometric parameters are nondimensionalized with respect to one-half the thickness t_C of the center adherend. The thickness of the center adherend, $2t_C$, is constant in all the parametric studies. The overhang length b is nondimensionalized with respect to the overlap length c. The ranges of the absolute magnitudes of the parameters and the nondimensionalized magnitudes are given in Table 2.

Influence of E_M/E_A

The shear distribution at the interfaces with the center adherend, $x=X_1$, is shown in Fig. 2 for three values of

Table 2 Magnitudes of parameters of analysis[a]

Joint parameter	Absolute magnitude Minimum mm (in.)	Absolute magnitude Maximum mm (in.)	Nondimensional form Parameter[b]	Nondimensional form Magnitudes
Length of overlap, c	13(0.5)	102(4.00)	c/t_C	1.02, 1.52, 2,3, 4.02, 5,6,8
Adhesive thickness, t_A	1.5(0.06)	11.7(.46)	t_A/t_C	0.12, 0.32, 0.52, 0.74, 0.92
Outer adherend thickness, t_O	6.4(0.25)	25.4(1.00)	t_O/t_C	0.5, 1.0, 1.5, 2.0
Length of overhang, d	0	102(4.00)	d/c	0, 0.99, 1.49, 1.99, 2.20, 4.57

[a]The notation is shown in Fig. 1. [b]t_C is one-half the thickness of the center adherend.

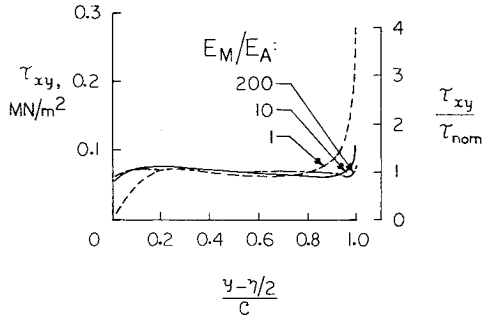

Fig. 2 Shear stress distribution in adhesive along $x=X_1$ for three values of E_M/E_A.

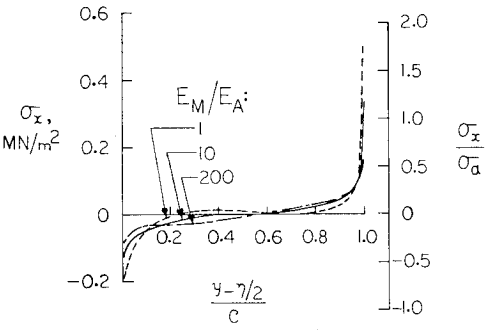

Fig. 4 Tear stress distribution in adhesive along $x=X_1$ for three values of E_M/E_A.

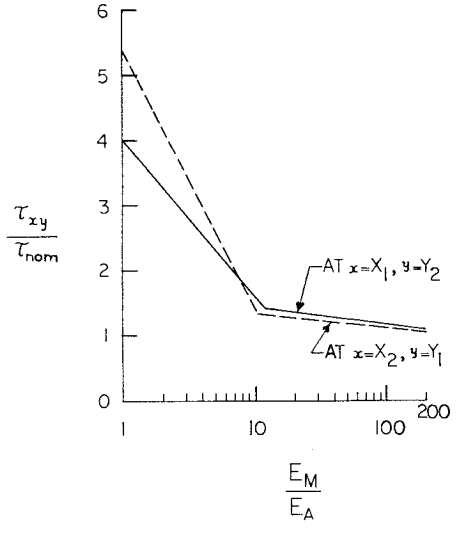

Fig. 3 Shear stress concentration factor vs E_M/E_A.

E_M/E_A. The maximum shear stress, and hence the scf, at each interface occurs 0.125 mm (.005 in.) from the respective leading end of the adherend. The magnitude of the shear stress decreases rapidly away from the leading end and is almost uniform and equal to the nominal shear stress over the middle two-thirds of the overlap. The shear stress then drops to zero at the trailing end of the interface. As E_M/E_A increases, the shear scf decreases, and the shear stress is uniform over an increasing length in the middle of the overlap. The variations in the shear scf at the center and outer adherends with respect to E_M/E_A are given in Table 3. A graphical representation of this variation is shown in Fig. 3. The magnitude of the highest shear stress in the adhesive is greater at the outer adherend than at the center adherend for values of $E_M/E_A<7.5$. The maximum shear stresses are almost equal to one another and to the nominal shear stress for $E_M/E_A=200$.

The reduction in the shear scf gained when $E_M/E_A>40$ is marginal.

The distribution of the tear stresses in the adhesive along the interface with the center adherend is shown in Fig. 4 for three values of E_M/E_A. The tear stresses are tension at the leading end of the interface and compression at the trailing end. Over the middle two-thirds of the overlap, the tear stresses are nearly uniform and almost zero in magnitude. The values of the tensile scf at both interfaces are given in Table 3 and graphically shown in Fig. 5. The tear scf is greatest for $E_M=E_A$. From Figs. 2 and 4, we see that the absolute magnitudes of the maximum tear stress are greater than the maximum shear stress in this joint geometry for all values of E_M/E_A. The tear failure of the adhesive will then be the criterion governing failure because adhesives are weaker in tension than in shear.

The distribution of the axial normal stress along the interfaces with the center and outer adherends is shown in Figs. 6 and 7, respectively. The distribution in the center adherend has a peak just beyond $y=Y_2$. The magnitude of the axial normal stress then drops rapidly in the overhang region and becomes equal in magnitude to the applied stress at one-half the overlap length beyond $y=Y_2$. The highest magnitude in the axial normal stress distribution in the outer adherend occurs at a point just outside the leading end of the interface. At the trailing ends of the adherends, the axial normal stress is zero. The magnitude of the peak axial normal stress occurs at $E_M=E_A$. The variations of the axial normal scf for the center and outer adherends is shown in Fig. 8. In the center adherend, this scf is almost constant at 1.60 for values of $E_M/E_A>20$. In the outer adherend, this scf is lowest at 3.43 for $E_M/E_A=20$. The magnitudes of the axial normal scf are also given in Table 3.

Influence of Overlap Length

The distribution of the nondimensionalized shear stress in the adhesive along $x=X_1$ is shown in Fig. 9. The shear scf is almost the same for all the overlap lengths analyzed in this

Table 3 Stress concentration factors for various values of E_M/E_A

	Stress concentration factors					
	Shear stress[a]		Tear stress[b]		Axial normal stress[c]	
E_M/E_A	Center adherend	Outer adherend	Center adherend	Outer adherend	Center adherend	Outer adherend
1	4.00	5.48	1.75	1.35	2.52	5.39
2	3.25	4.26	1.52	1.32	2.16	4.58
4	2.51	3.00	1.38	1.12	1.91	3.99
10	1.60	1.34	1.25	0.88	1.73	3.55
20	1.34	1.18	1.19	0.75	1.67	3.43
200	1.10	1.08	1.10	0.64	1.60	4.16

[a]The shear stress concentration factor is calculated in the adhesive with respect to the nominal shear stress. [b]The tear stress concentration factor is calculated in the adhesive with respect to the applied stress. [c]The axial normal stress concentration factor is calculated in the adherends with respect to the applied stress.

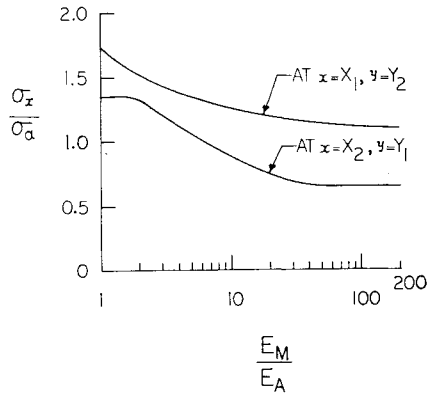

Fig. 5 Tear stress concentration factor vs E_M/E_A.

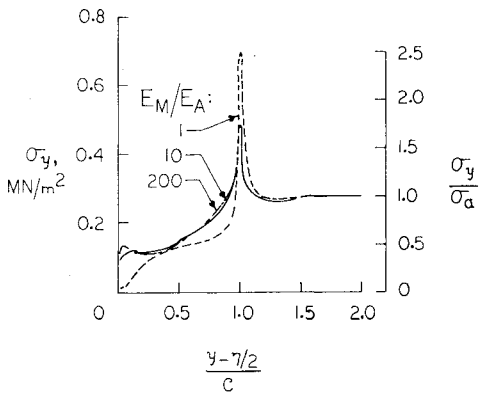

Fig. 6 Axial normal stress distribution in center adherend along $x=X_1$ for three values of E_M/E_A.

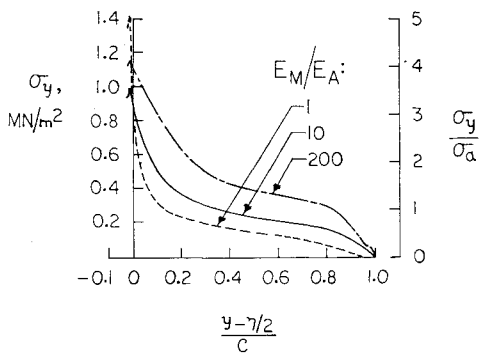

Fig. 7 Axial normal stress distribution in outer adherend along $x=X_2$ for three values of E_M/E_A.

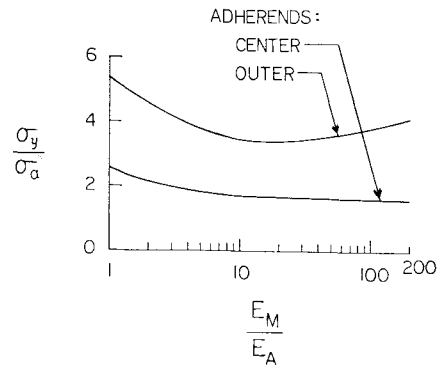

Fig. 8 Axial normal stress concentration factor in center and outer adherends vs E_M/E_A.

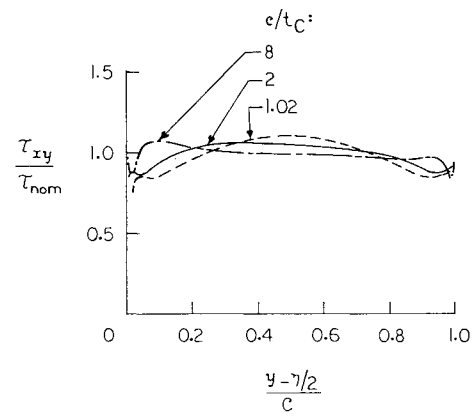

Fig. 9 Shear stress distribution in adhesive along $x=X_1$ for three overlap lengths.

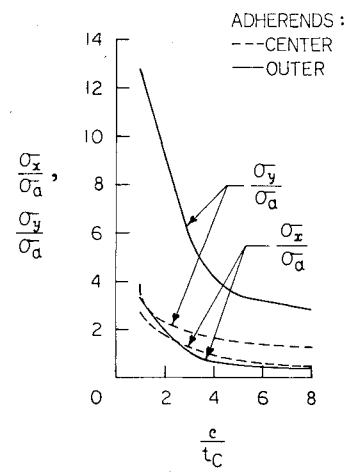

Fig. 10 Tear stress and axial normal stress concentration factor vs overlap length.

study. The shear stress distribution is almost uniform for $c/t_C=2.00$. The most obvious feature of the distributions is the location of the maximum shear stress. For $c/t_C=1.02$, the maximum shear stress occurs at the middle of the overlap length. As c/t_C increases, the position of the maximum shear stress approaches the leading end of the interface. The shear stress distribution with the outer adherend is similar to that shown in Fig. 9.

The variations of the tear scf with overlap length are shown in Fig. 10. The maximum tear stresses occur at the ends of the overlap adjacent to the leading ends of interfaces. The tear stresses at the outer adherend are higher than those at the center adherend for $c/t_C<2$. The advantage gained in scf for $c/t_C>4$ is marginal.

The variations in the axial normal scf with length of overlap are also shown in Fig.10 for the center and outer adherends. The maximum axial stresses occur when the overlap length is shortest, i.e., when $c/t_C=1.00$. The magnitude of the axial normal scf at the outer adherend is three times greater than that at the center adherend for all values of c/t_C. As c/t_C increases, this scf decreases rapidly until the advantage gained with longer overlap lengths is marginal for $c/t_C>5$.

Influence of Outer Adherend Thickness

The influence of the variation in the thickness of the outer adherend on the shear stress and the tear stress concentration factors is marginal. The variation in their magnitudes is barely discernible. The variation in the axial normal scf on the outer adherend is most prominent and is shown in Fig. 11.

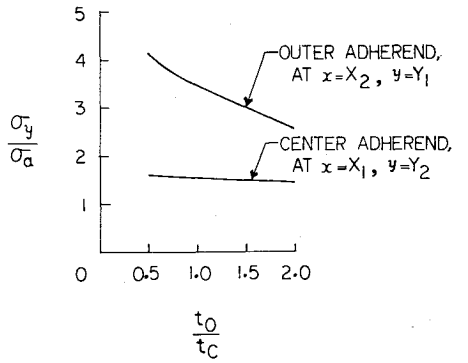

Fig. 11 Axial normal stress concentration factor in center and outer adherend vs t_O/t_C.

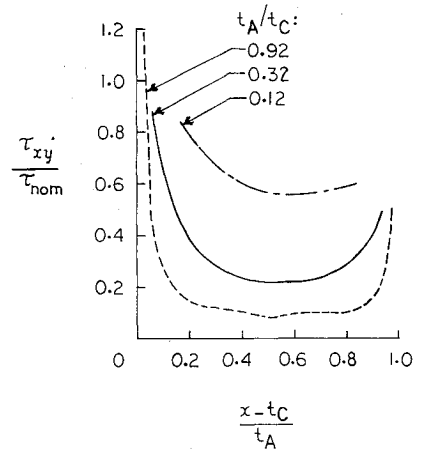

Fig. 12 Shear stress distribution through adhesive thickness at $y = Y_2 - 0.25$ mm for three values of t_A/t_C.

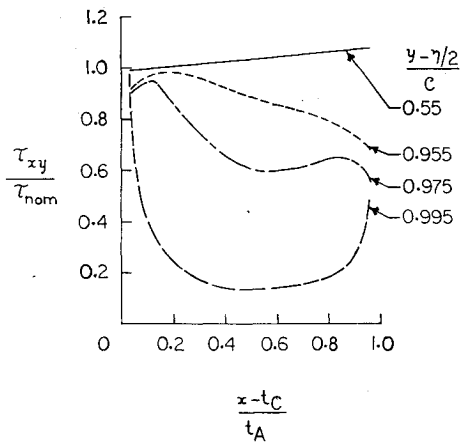

Fig. 13 Shear stress distribution through adhesive thickness at four locations along the overlap.

The variation in the axial normal scf on the center adherend is negligible. For small values of t_O/t_C, the axial normal scf on the outer adherend is 4 and drops rapidly as t_O/t_C increases. This drop continues beyond $t_O/t_C = 2.00$, the maximum magnitude of this nondimensionalized parameter examined in this study.

Influence of the Adhesive Thickness

The distributions of the nondimensionalized shear stresses through the adhesive at $y = Y_2 - 0.25$ mm for three thicknesses of the adhesive are shown in Fig. 12. The distributions are increasingly nonuniform as the adhesive thickness increases

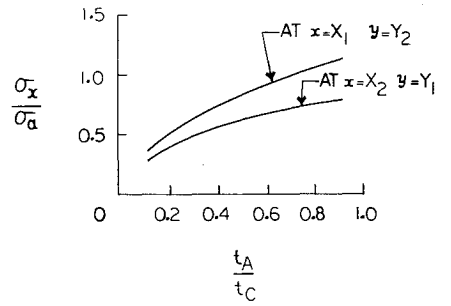

Fig. 14 Tear stress concentration factor at center and outer adherends vs t_A/t_C.

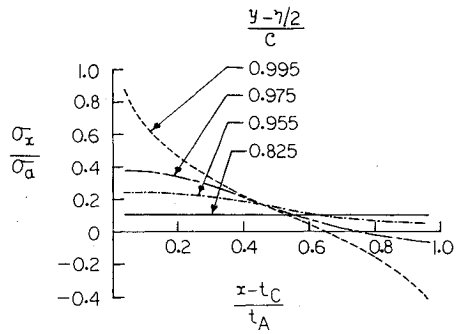

Fig. 15 Tear stress distributions through adhesive thickness at four locations along the overlap.

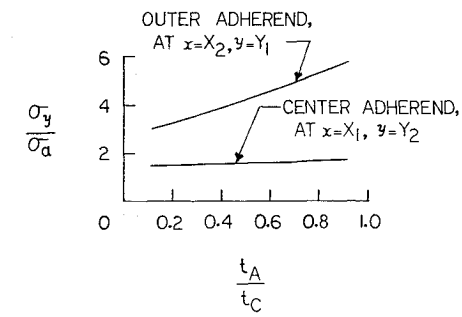

Fig. 16 Axial normal stress concentration factor in center and outer adherends vs t_A/t_C.

with peaks at the interfaces. This behavior results in steeper stress gradients near the interfaces and higher shear scf with increase in adhesive thickness. The nondimensionalized shear stress distributions through the adhesive thickness at four locations along the overlap length of the reference joint are shown in Fig. 13. Near the middle of the overlap, i.e., at $(y - \eta/2)/c = 0.55$, the shear stress is almost uniform and of the magnitude of the nominal shear stress. As the ends of the overlap are approached, the shear stress distribution becomes increasingly nonuniform.

The tear scf increases with increasing adhesive thickness. This variation is shown in Fig. 14. The tear scf is greater at the center adherend than that at the outer adherend and is increasingly greater as t_A/t_C increases for this geometry of the overlap length. The variation in the tear stress distribution at four locations along the overlap length of the reference joint is shown in Fig. 15. The tear stress is zero at the middle of the overlap. Over the middle two-thirds of the overlap length, the tear stress distribution is uniform. As the ends of the overlap are approached, this distribution becomes increasingly nonuniform and is tension at the leading end of one adherend and compression at the trailing end of the other adherend.

The variation of the axial normal scf in the adherends with variation in the adhesive thickness is shown in Fig. 16. The

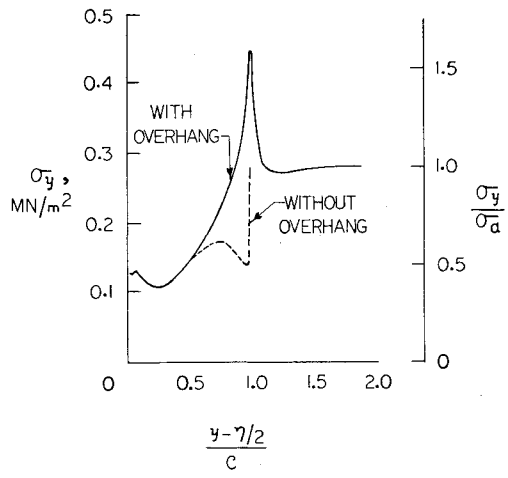

Fig. 17 Axial normal stress distribution in center adherend along $x = X_1$ for joints with and without overhang.

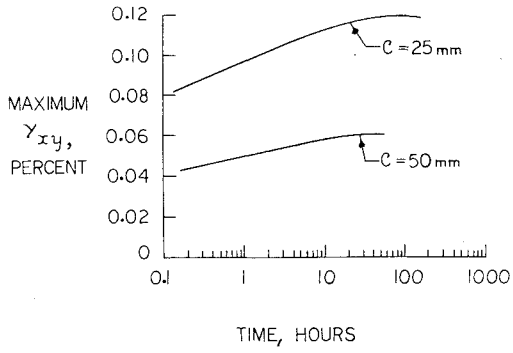

Fig. 18 Maximum creep shear strain in the adhesive along $x = X_1$ vs time.

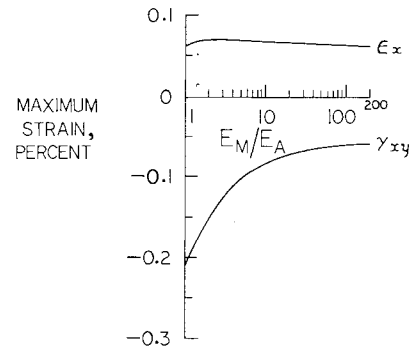

Fig. 19 Maximum shear and tear strains vs E_M/E_A at time $t = 16.67$ h.

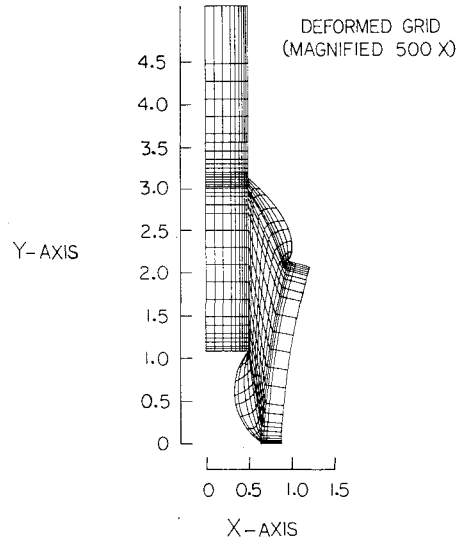

Fig. 20 Deformed finite element grid for the reference joint with displacements magnified 500 times.

influence on the center adherend is negligible, but the axial normal scf on the outer adherend increases almost linearly with increase in adhesive thickness.

Influence of Overhang Length

The joint shown in Fig. 1 is subjected to a uniform distributed stress on the center adherend at the free end of the overhang which is some distance away from the leading end of the interface. If the load is distributed in line with the leading end, then the change in the adherend stresses would be very pronounced. The axial normal stress distribution along $x = X_1$ of the reference joint with and without overhang is shown in Fig. 17. The magnitude of the highest axial normal stress in the joint with overhang is 50% higher than in the joint without overhang. The erroneous idealization of applying the load in the center adherend in line with the leading end becomes obvious in studying the strain distributions in double-lap joints with and without overhang. Although the joint with overhang can fail by yielding of the center adherend, the joint without overhang will probably fail because of separation (tear) of the adhesive from the center adherend.

Creep Strain in the Adhesive

The stress analysis presented in this study is of a joint bonded with a viscoelastic adhesive and subjected to a constant load for a long period of time. The failure in the joint can, therefore, be caused by large strains in the adhesive even though the stresses remain constant. Two joints are compared in this phase of the study: the reference joint where the overlap length is 50 mm and a second joint with an overlap length of 25 mm but with all other parameters remaining the same as in the reference joint. The timewise variation in the maximum shear strain, γ_{xy}, in the adhesive is shown in Fig. 18. The variations are for the strains in the center adherend-adhesive interface. The creep shear strain increases monotonically with time for the first 50 h, after which the rate of increase decreases, and the curves become flat. The creep strain after 50 h is 70% greater than the initial strain. The timewise variation of the creep shear strain is similar. The variations in the shear and tear strains with E_M/E_A, 16.67 h after loading, are shown in Fig. 19. The creep tear strain increases marginally with decrease in E_M/E_A, but the creep shear strain at $E_M/E_A = 1$ is 3.5 times greater than that at $E_M/E_A = 200$.

The influence of creep strain can be better understood by studying the deformation of the joint. The deformed finite element grid of the reference joint five hours after loading is shown in Fig. 20. The displacements in this deformed grid are magnified 500 times. The displacement in the center adherend is almost entirely in the y direction. The displacements in the adhesive are such that the free edges bulge out as if they were subjected to compression displacements in the x direction. The bulge disappears within 4% of the overlap length from the free edges. The adhesive is subjected to tension tear displacements $+u_x$ and compression axial displacements $-u_y$ at the interface leading ends. At the interface trailing ends, the signs of the corresponding displacements are interchanged. The adhesive displacements are so large that the outer adherend is subjected to bending, with displacement u_x in the outer adherend increasing with increasing y. As the applied load is increased or the overlap length is decreased, the influence of the creep strain as the failure criterion will be increasingly important.

Joint Design

In the design of a double-lap joint, several options are available in choosing the magnitudes of the parameters of an efficient joint. The results are presented in non-dimensionalized form with respect to the center adherend thickness. Thus, the admissible design axial normal stress in the center adherend and the design nominal shear stress can be used as criteria for the first estimate of the center adherend thickness and the overlap length. The first estimate can then be re-evaluated, and accordingly modified, on gaging the influences of the other joint parameters.

The most important parameter is the ratio E_M/E_A. This ratio should be greater than 10 in order for the shear stress to be of low magnitude. The magnitude of the shear stress is not appreciably influenced by the geometry of the joint provided the nominal shear stress is within admissible limits. The adhesive thickness must be small in order for the shear stress gradients at the interfaces to be small. The overlap length for a uniform shear stress distribution should be equal to the total thickness of the center adherend. However, this restraint on the overlap length could result in high tear stresses in the adhesive and high axial normal stresses in the adherends.

To reduce the high tear stresses in the adhesive, the overlap length should be such that $c/t_C > 5$ and $E_M/E_A > 40$, which in turn will further reduce the shear stresses. The influences of the outer adherend thickness and the adhesive thickness on the tear stresses are negligible, although a thin adhesive will further reduce the tear stresses.

The failure of the center adherend can be caused by high axial normal stress occurring near the leading end of the interface. This stress will be nearly a minimum if $E_M/E_A > 40$ and $c/t_C > 5$. The outer adherend thickness and the adhesive thickness have negligible influence on the magnitudes of this stress.

The axial normal stress in the outer adherend is a minimum when $E_M/E_A = 20$. The overlap length has a strong influence on this stress, and a ratio of $c/t_C > 5$ must be maintained. The influence of the outer adherend thickness is considerable, and $t_O/t_C > 2$ is desirable. The adhesive thickness should be as small as possible in order to further reduce the magnitude of the axial normal stress in the outer adherend.

The influence of the geometry on the creep tear and shear strains is similar to that on the tear and shear stresses. That is, the stresses must be small in order for the initial strain to be low. At long times, strains can creep to an additional 70% of the initial strain. The ratio E_M/E_A must be greater than 40 in order for the initial strain to be low.

A simple nondimensionalized overlap ratio with adherends of identical materials is suggested:

$$\Omega = \sqrt{(c^2 E_A t_A / E_m t_O t_C^2)}$$

where t_A is the adhesive thickness, t_C is the center adherend thickness, t_O is the outer adherend thickness, c is the overlap length, E_M is the adherend modulus, and E_A is the representative adhesive modulus. The maximum tear stresses at the center and outer adherends are equal when $\Omega = 0.15$. For $\Omega < 0.15$, the tear stress at the outer adherend is greater than that at the center adherend. For $\Omega = 1.5$, the maximum shear stresses at the outer and center adherends are equal. For $\Omega > 1.5$, the increase in the maximum shear stress is monotonic, with that in the outer adherend being greater than that at the center adherend. In our analysis, we find that the double-lap joint is efficient when $E_M/E_A = 40$, $c/t_C = 5$, $t_A/t_C = 0.1$, and $t_O/t_C = 2$, where $\Omega = 0.177$. This magnitude of Ω will be greater if the stresses are lowered further by a larger overlap length. Or, Ω will be lower if E_M/E_A is greater than 40 or if $t_O/t_C > 2$ or $t_A/t_C < 0.1$ in attempts to reduce the stress concentration factors.

Concluding Remarks

The double-lap joint, bonded with a viscoelastic adhesive, can be analyzed such that the stress distributions in the adhesive and adherends are determined as a function of time. In this study, the importance of considering the adhesive of finite thickness with the stresses varying across the adhesive thickness is demonstrated. In addition, the influence of creep strains on the probable failure mode of the joint is shown. The effects on the stress distributions, and consequently the failure mode, caused by idealization of the joint by previous investigators are also described. The quantitative influences of the various geometric and material parameters are demonstrated. Based on these parameters, an overlap ratio is introduced for joints with identical adherend materials. The efficiency of the joint can be estimated by use of the overlap ratio. This overlap ratio can also be used to predict at which of the adherends the adhesive tear and shear stresses will have the larger magnitude.

References

[1]Crose, J.G. and Jones, R.M., "SAAS III, Finite Element Stress Analysis of Axisymmetric and Plane Solids with Different Orthotropic Temperature-Dependent Material Properties in Tension and Compression," The Aerospace Corp., San Bernardino, Calif., Aerospace Rept. No. TR-0059(S6816-53)-1, June 1971.

[2]Schapery, R.A., "Approximate Methods of Transform Inversion for Viscoelastic Stress Analysis," *Proceedings of Fourth U.S. National Congress on Applied Mechanics*, 1962, Vol. 2, pp. 1075-1085.

[3]Sen, J.K. and Jones, R.M., "Stress Analysis of Double-Lap Joints Bonded with a Viscoelastic Adhesive, Part I: Theory and Experimental Corroboration," *AIAA Journal*, Vol. 18, Oct. 1980, pp. 1237-1244.

[4]Sen, J.K., "The Mechanical and Optical Characterization of a Linear Viscoelastic Material," presented at SESA Spring Meeting, Dallas, Texas, May 15-20, 1977.

[5]Sen, J.K., "Stress Analysis of Double-Lap Joints Bonded with a Viscoelastic Adhesive," Ph.D. Dissertation, Dept. of Civil and Mechanical Engineering, Southern Methodist University, Dallas, Texas, May 1977. Available from Xerox University Microfilms International, 300 N. Zeeb Road, Ann Arbor, Mich. 48106 as Order No. 77-18,606.